The Astrophysical Journal Letters, 969:L35 (6pp), 2024 July 10 https://doi.org/10.3847/2041-8213/ad5962

The Colocation of Magnetic Reconnection and Current Disruption in Jovian Middle Magnetosphere

Dong-Xiao Pan[1], Zhong-Hua Yao[2,3], Rui-Long Guo[4], Christopher S. Arridge[5], Licia C. Ray[5], Yong Zhao[3], George Clark[6], I. Jonathan Rae[7], Anthony T. Y. Lui[6], Bin-Zheng Zhang[2], Yong Wei[3], Xu-Zhi Zhou[8], Hui-Shan Fu[9], John E. P. Connerney[10,11], and Scott J. Bolton[12]

[1] School of Geophysics and Information Technology, China University of Geosciences (Beijing), Beijing, People's Republic of China
[2] Department of Earth Sciences, The University of Hong Kong, Hong Kong SAR, People's Republic of China; yaozh@hku.hk
[3] Key Laboratory of Earth and Planetary Physics, Institute of Geology and Geophysics, Chinese Academy of Sciences, Beijing, People's Republic of China
[4] Laboratory of Optical Astronomy and Solar-Terrestrial Environment, Institute of Space Sciences, School of Space Science and Physics, Shandong University, Weihai, Shandong, People's Republic of China
[5] Department of Physics, Lancaster University, Lancaster, UK
[6] Applied Physics Laboratory, Johns Hopkins University, Laurel, MD, USA
[7] Northumbria University, Newcastle upon Tyne, UK
[8] School of Earth and Space Sciences, Peking University, Beijing, People's Republic of China
[9] School of Space and Environment, Beihang University, Beijing, People's Republic of China
[10] Space Research Corporation, Annapolis, MD, USA
[11] NASA Goddard Space Flight Center, Greenbelt, MD, USA
[12] Southwest Research Institute, San Antonio, TX, USA

Received 2024 May 14; revised 2024 June 17; accepted 2024 June 17; published 2024 July 9

Abstract

Magnetic reconnection and current disruption are two key processes in driving energy conversion and dissipation in planetary magnetospheres. At the Earth, the two processes usually occur at different locations: the current disruption process occurs more frequently in the near-Earth magnetotail $\sim 10\,R_E$, while the magnetotail reconnection process is expected to take place in the more distant region where the current sheet is thinner. Occasionally, under very intense solar wind perturbations, reconnection could be located closer to the Earth where current disruption processes usually operate. But it is unclear what the situation is at giant planets, in which the plasma environment is very different from the Earth. In this study, we investigate a middle-Jupiter reconnection event at $\sim 43\,R_J$. During the event, the inferred integrated cross-field currents were substantially reduced, which we argue is a signature of current disruption. In this case, we suggest that magnetic reconnection could be colocated with a current disruption process in the Jovian magnetosphere, which is roughly analogous to the situation in the extremely perturbed Earth's magnetosphere.

Unified Astronomy Thesaurus concepts: Planetary magnetospheres (997)

1. Introduction

Magnetic reconnection, a local change in the topology of magnetic field lines, occurs throughout the Universe, for example in planetary systems (e.g., Huddleston et al. 1997; Zarka 2007), galaxy clusters (e.g., Makishima 2001), and also laboratory plasma environments (e.g., Zweibel & Yamada 2009). It is a key process that significantly energizes charged particles by converting magnetic energy into kinetic and wave energy. In planetary magnetospheres, the magnetic reconnection plays an important role in energy and mass circulation, and many magnetospheric phenomena are relevant to magnetic reconnection processes, e.g., magnetic dipolarizations, auroral emissions, and plasma waves.

Magnetic reconnection events are usually identified in magnetospheric current sheets. If the oppositely directed magnetic fields become the dominant components in a region of the current sheet, magnetic reconnection could be triggered (Dungey 1961; Paschmann et al. 1979). In the terrestrial magnetosphere, the condition of oppositely directed magnetic field is easy to be fulfilled at the magnetopause (e.g., Sonnerup 1974) and mid-magnetotail neutral sheet at $\sim 20-30\,R_E$ (e.g., Angelopoulos et al. 2008), and thus magnetic reconnection processes are frequently identified in these regions. Instead, in the near-Earth magnetotail ($\sim 10\,R_E$ or inner-magnetosphere), the magnetic field configuration is more dipole-like and reconnection is not expected to take place.

Current disruption occurs in the near-Earth magnetotail, changing the magnetic field line from a stretched to a more dipolar configuration (e.g., Lui 2002). The near-Earth magnetic current disruption and mid-magnetotail magnetic reconnection are physically connected, and both of them are fundamental energy release processes in planetary magnetospheres. The sequence of near-Earth current disruption and mid-tail reconnection has been debated for more than 20 yr (e.g., Lui 1996; Ohtani 2001; Angelopoulos et al. 2008; Lui 2009; Pu et al. 2010), but there has been little doubt that these processes are spatially separated. However, the near-Earth reconnection events, located at $<10\,R_E$, have been reported during intense geomagnetic storms caused by very strong solar wind perturbations (Miyashita et al. 2005; Angelopoulos et al. 2020). These findings substantially reshaped the limit of conditions for reconnection in the terrestrial magnetosphere, but, it is not yet known whether such an understanding could be applied to giant planetary magnetospheres, where the plasma environment is very different from Earth.

In contrast to Earth, the Jovian magnetospheric system is strongly influenced by internal sources of energy, mass, and momentum. The dynamics of the Jovian magnetosphere are mainly influenced by rapid planetary rotation, while the moon Io provides continuous plasma to the system as a major contributor (Vasyliunas 1983; Krupp et al. 2004; Kivelson & Southwood 2005). Ultimately, this mass provided by the moons must be lost from the system, with possible mechanisms including magnetic reconnection leading to the release of plasmoids (Vogt et al. 2014; Delamere et al. 2015; Sarkango et al. 2021, 2022). Using data from the Galileo and Juno spacecraft, previous studies have identified hundreds of reconnection events in the Jovian magnetosphere (Vogt et al. 2010, 2020). These reconnection events suggest a statistical X-line, located between $\sim 60\,R_{\rm J}$ and $\sim 90\,R_{\rm J}$, although signatures of reconnection could still be identified in the middle magnetosphere (e.g., $<50\,R_{\rm J}$; Russell et al. 1998, 1999; Vogt et al. 2020). Since magnetic reconnection could take place in the middle magnetosphere (roughly the region connecting to Jupiter's main aurora), it is intriguing whether the magnetic reconnection process could drive dynamical electric currents which couple Jupiter's magnetosphere and ionosphere.

In this study, we analyze a magnetic reconnection event observed by Juno at $\sim 43\,R_{\rm J}$ and specifically examine the variation in cross-field currents. We suggest that this reconnection is colocated with a current disruption process. This result provides a new understanding of fundamental processes for energy release in rotationally driven magnetospheres.

2. Observations

Figure 1 presents an overview of measurements from 2017 May 15–16 and shows measurements of the magnetic field from the Magnetic Field Investigation (MAG) instrument (Connerney et al. 2017), energy spectrum for 30 keV–1 MeV energetic electrons from the Jupiter Energetic Particle Detector (JEDI) Instrument (Mauk et al. 2017), and 100 eV–100 keV electrons from the Jovian Auroral Plasma Distributions Experiment (JADE) instrument (McComas et al. 2017). The magnetic fields are recorded in Jupiter-De-Spun-Sun (JSS) coordinates in spherical polar representation, where $\hat{\mathbf{e}}_r$ is a radial vector directed from the planet to the spacecraft, $\hat{\mathbf{e}}_\theta$ is the polar vector based on Jupiter's rotation axis, and $\hat{\mathbf{e}}_\phi$ is oriented in the azimuthal direction and completes the right-handed set.

The magnetic field B_r and B_ϕ components, shown in Figures 1(a) and (c), typically vary with a 10 hr periodicity. This period corresponds to the current sheet flapping due to the fast rotation of the planet and the fact that the magnetic dipole is tilted. The electron fluxes increase when Juno approaches the central magnetodisc (see Figure 1(e)). An intense disturbance is observed from 01:00 UT to 03:00 UT on May 16. At $\sim$02:10 UT, there is a B_θ bipolar event (marked with the pink shaded area), which could also be related to auroral dawn storms and injection processes (Yao et al. 2020). This event is located in the dawn sector of Jupiter's magnetosphere around 4.5 local time, about 6° north of Jupiter's equatorial plane, and at a radial distance of $\sim 43\,R_{\rm J}$. The B_θ bipolar signature is accompanied by an enhancement of electron intensities with energies up to hundreds of keV. These electrons are more energetic than those during a previous plasma sheet crossing (e.g., at $\sim$02:00 UT on May 16), indicating a strong plasma energization process. We demonstrate later that this B_θ bipolar event, accompanied by plasma energization, is a signature of magnetic reconnection. Around 02:30 UT the magnetic fields show a strong B_r decrease and such a magnetic field variation has been identified as a magnetic dipolarization (Yao et al. 2020).

The magnetic field in the magnetodisc is generally swept back due to currents flowing both azimuthally and radially in the magnetodisc. To better understand the reconnection process, we transformed the magnetic field data from JSS coordinates to an X-line coordinate system. The *X*-direction is almost along the background magnetic field, the *Z*-direction is almost parallel to Jupiter's spin axis (positive to northward), and the *Y*-direction is perpendicular to the plane of the swept-back magnetic field, completing the right-handed set. The X-line frame is obtained using the interval between 03:00 UT and 03:30 UT where the magnetic fields were not highly perturbed (Arridge et al. 2016; Guo et al. 2018). Figures 2(a)–(d) show the magnetic field data in X-line coordinates, an inferred trajectory of Juno in the reconnection diffusion region in Figure 2(e), and measured electron pitch-angle distributions from JEDI in Figures 2(f) to (i).

Juno was located northward of the central magnetodisc ($B_x > 0$) when it detected this event (Figure 2(b), region 1). The B_z component reverses at $\sim$02:09:50 UT (from northward $\sim$10 nT to southward ~ -10 nT), which indicates that Juno crossed the X-line from antiplanetward side to planetward side. The four pitch angle versus energy distributions are sampled from the background environment (Figure 2(f)), antiplanetward of the X-line region (Figure 2(g)), planetward of the X-line region (Figure 2(h)), and the background magnetosphere with more energetic electrons (Figure 2(i)). Each electron pitch-angle distribution is obtained by averaging data during the selected time interval (labeled on the top of the corresponding plot). Figure 2(f) shows an isotropic electron distribution in the background plasma environment. Distributions in Figures 2(g) and 2(h) are from opposite sides of the X-line. They are both asymmetric, and the sense of the asymmetry reverses across the X-line: on the antiplanetward side, the parallel population (0° pitch angle) dominates (Figure 2(g)) whereas on the planetward side, the antiparallel populations (180° pitch angle) are slightly larger than the parallel populations (Figure 2(h)). The bistreaming distributions on both sides of the reconnection site imply that the magnetic field line is not open to interplanetary space. Finally, the electron distributions become isotropic again, but with higher energies than Figure 2(f), which indicates that the Juno spacecraft is back to the background environment (Figure 2(i)).

These signatures provide strong evidence that Juno was measuring an ongoing reconnection process in the middle magnetosphere on the dawnside. The exact motion of the X-line is difficult to determine because of the single-spacecraft nature of the measurements. The motion of the spacecraft across the X-line may be because the X-line is corotating with the planet, as observed in Saturn's magnetosphere (Yao et al. 2017), or may be due to magnetodisc flapping (Russell et al. 1999; Volwerk et al. 2013; Martin & Arridge 2017), or the X-line retreating away from the planet (Arridge et al. 2016).

3. Discussion and Conclusion

Figure 3 presents a comparison between this reconnection event at Jupiter ($\sim 43\,R_{\rm J}$) and a near-Earth reconnection event at $\sim 8\,R_{\rm E}$ (Angelopoulos et al. 2020). The Jupiter event is linked to a dawn storm (Yao et al. 2020) and the Earth event is closely related to a substorm (Angelopoulos et al. 2020). The black

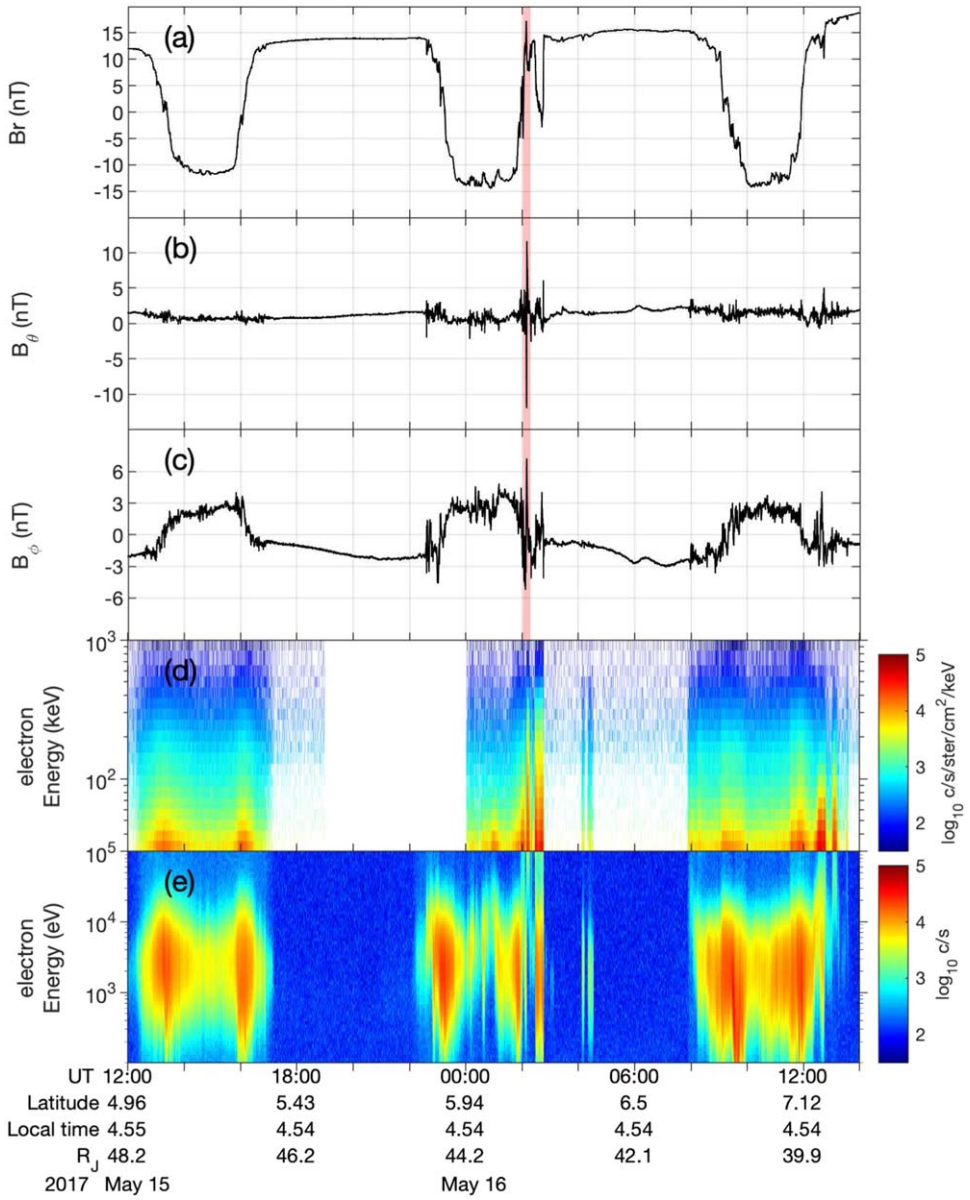

Figure 1. Overview of the magnetosphere between 12:00 UT on May 15 and 14:00 UT on May 16. (a)–(c) Three components of the magnetic field in Jupiter-De-Spun-Sun (JSS) coordinate; (d) and (e) electron energy spectrum from JEDI and JADE instrument. The pink shaded area marks the reconnection event.

lines in Figures 3(a) and (b) show the profiles of the north–south magnetic field components for these two events. Both of these events contain bipolar signatures followed by enhancements of the north–south component. The enhanced north–south magnetic field components are usually regarded as a consequence of current disruption. Furthermore, the decrease of B_r component for the Jupiter event and B_{lobe} for the Earth event (shown in red lines in Figure 3) are related to current reconfiguration processes (Lui 2011a; Yao et al. 2017). Therefore, we suggest that both of these events are colocated with current disruption.

We use the magnetic field measurements to estimate the change in the cross-field current density during current disruption. Figure 4(b) presents the B_x component (in X-line coordinates), which shows an overall decreasing trend following the crossing of the X-line. A decrease in B_x is often regarded as an indication of current reduction (Yao et al. 2019, 2020), although, because we only have observations from a single spacecraft, it is hard to rule out the possibility that this B_x decrease is due to complex magnetodisc motion, for example, a rippled or corrugated magnetodisc producing rapid vertical motions superimposed on regular magnetodisc flapping (Russell et al. 1999). However, as shown in Figure 4(b), the B_x variation before the reconnection event is relatively stable, and thus we suggest the B_x decrease is likely the manifestation of current reduction because magnetodisc motion usually corresponds to an obvious and quasiperiodic time variation in B_x. Moreover, this event is suggested to be associated with a dawn storm (Yao et al. 2020). Therefore, the steplike decrease of B_x, associated with the auroral dawn storm, is likely a consequence of cross-field current decrease that would naturally form field-aligned auroral currents to ensure the continuity of current.

If the magnetic variation of B_x (see Figure 4(b)), from $\sim$15 nT (before the reconnection) to $\sim$10 nT (after the reconnection), is due to current reduction, one could roughly estimate the current density embedded in the magnetodisc

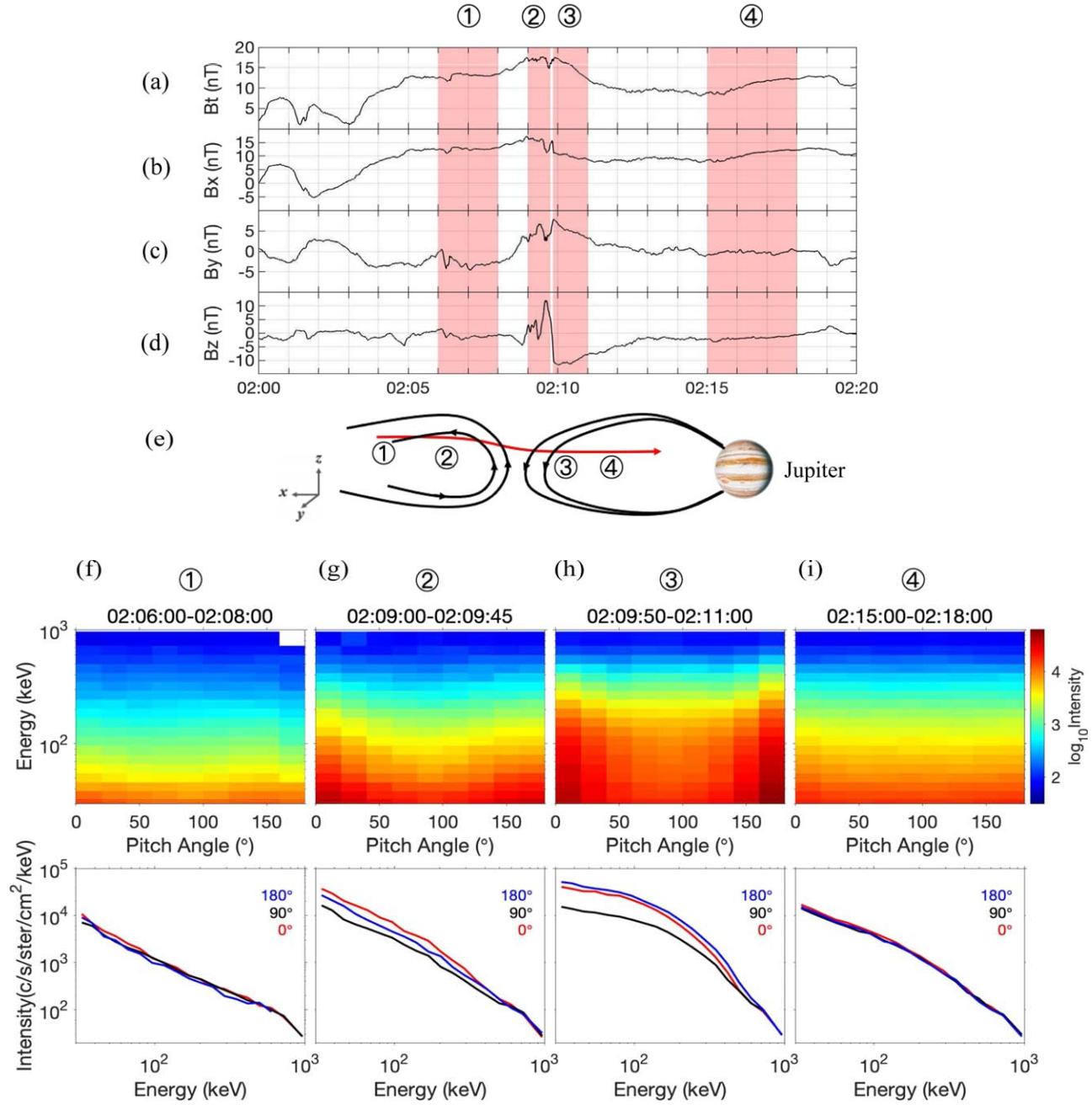

Figure 2. (a)–(d) Total magnetic field and three components of the magnetic field in the X-line coordinates between 02:00 UT and 02:20 UT on 2017 May 16, (e) an inferred trajectory of Juno relative to the geometry of the reconnection region, and (f)–(i) detected electron pitch-angle distributions at different regions.

current sheet based on Ampère's Law. In the calculation of current density, we assume that the observed magnetic field profile is well represented by a combination of a magnetic dipole and 1D current sheet. If the spacecraft is far from the center of the magnetodisc then $\frac{\partial}{\partial z} > \frac{\partial}{\partial x}, \frac{\partial}{\partial y}$ and the height-integrated current density over one hemisphere can be given by

$$I_y = \frac{1}{\mu_0}[B_x(z_j) - B_x(0)],$$

where $B_x(z_j)$ is the B_x component measured at Juno's position, and $B_x(0)$ represents the B_x component at the center of the magnetodisc (considered to be zero).

We highlight that the estimation of I_y may only be valid when the spacecraft is located in the outer plasma sheet or lobe region, where B_x is the dominant magnetic field component. In this case, the height-integrated current density I_y is a good estimate of the cross-field current density. The horizontal field angle, $\arctan(\sqrt{B_z^2 + B_y^2}/B_x)$ (see Figure 4(e)), is small when the B_x component dominates. Where this angle is less than 15°, we consider that I_y is a good estimate for the cross-field current density. The limit of 15° is an empirical choice to ensure enough data for further analysis. A different number does not change the patterns of the result.

Figure 4(f) shows the height-integrated/cross-field current density profile, in which the blue dots represent the part where the B_x dominant condition is satisfied. Since the height-integrated current density is sensitive to Juno's position, the calculated I_y would increase when the spacecraft is approaching

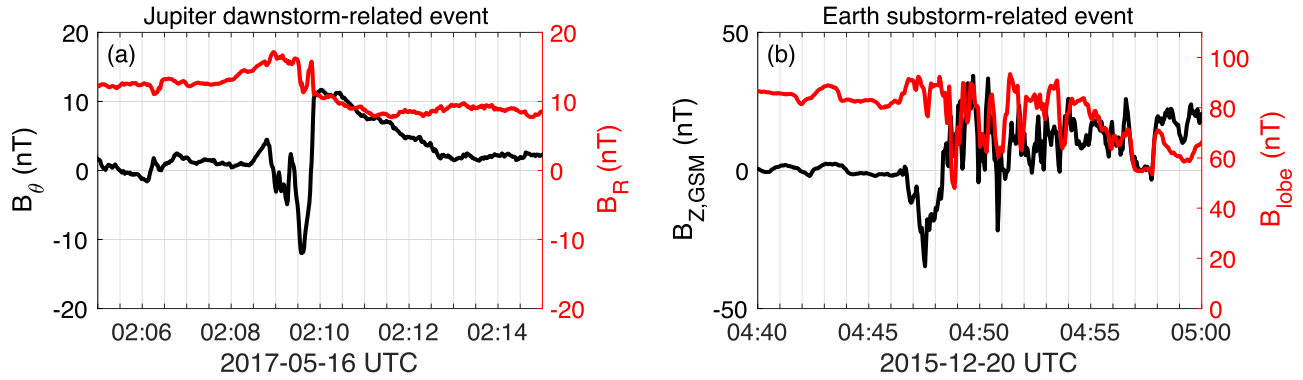

Figure 3. A comparison between the Jupiter dawn-storm-related event and Earth substorm-related event. (a) The magnetic field B_θ and B_R components (in Jupiter-De-Spun-Sun coordinate) for the Jupiter event on 2017 May 16, observed by Juno spacecraft. (b) The measurements of the magnetic field B_Z component (in Geocentric-Solar-Magnetospheric coordinate) for the Earth event on 2015 December 20 by THEMIS P5, and $B_{\rm lobe}$, inferred from total plasma pressure at P5 assumed to be in pressure balance with the lobe (magnetic) pressure (Angelopoulos et al. 2020).

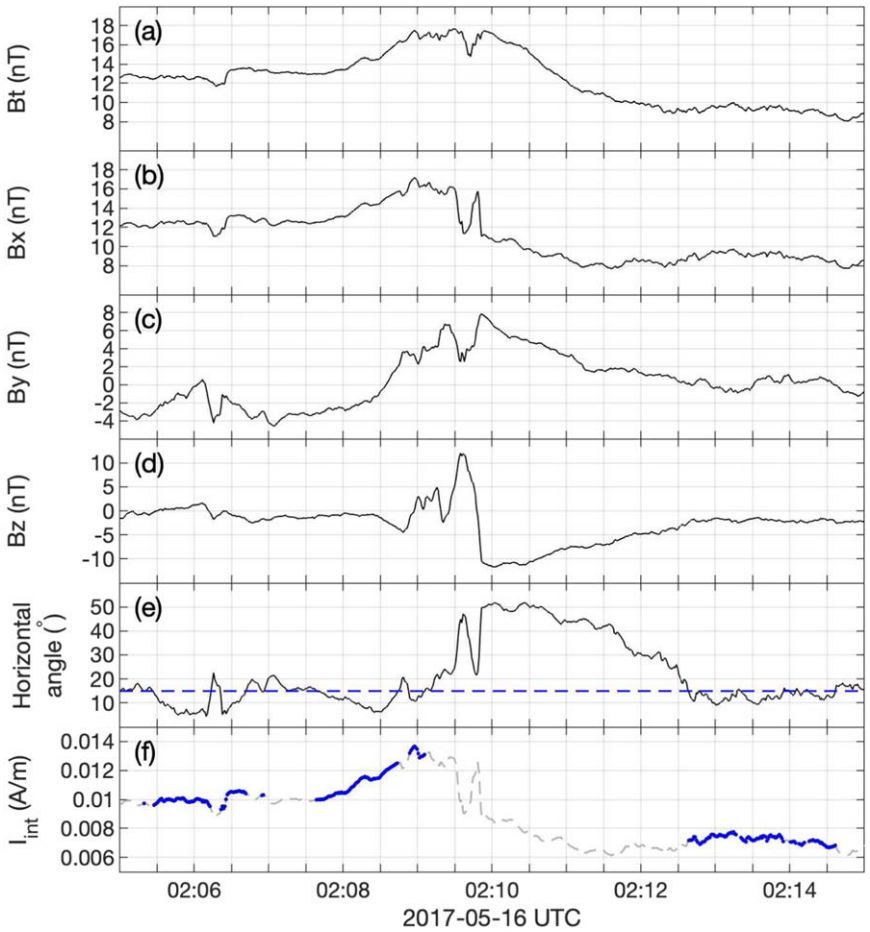

Figure 4. Overview of Juno spacecraft observations from 02:05 UT to 02:15 UT on 2017 May 16. (a)–(d) Magnetic field B_t (total field) and magnetic field components B_x, B_y, and B_z in the X-line coordinates. (e) Horizontal angle, defined as $\arctan(\sqrt{B_z^2 + B_y^2}/B_x)$. The dashed line represents the horizontal angle equal to 15°. (f) The currents integrated from the center of the magnetodisc to the satellite position; the blue dots represent where the magnetic field B_x dominates, corresponding to horizontal angles less than 15°.

the northern lobe. However, I_y is observed to decrease from $\sim$0.012 A m^{-1} (similar to the magnetodisc current density found by Lorch et al. 2020) to $\sim$0.007 A m^{-1} and is likely a sign of cross-field current disruption.

The reduction of cross-field current in the magnetosphere may indicate current diversion, in consideration of the closure of the currents. If we assume that the reduction part of the cross-field current ($\sim$0.005 A m^{-1}) corresponds to the field-aligned current that connects the magnetosphere and upper atmosphere/ionosphere (Cowley & Bunce 2001; Hill 2001; Southwood & Kivelson 2001), the integration of this field-aligned current over a dynamically disturbed region, for example, 2 R_J, is estimated to be around 1 MA. If a similar pattern occurred over a larger area, the field-aligned currents would be more intense and may even be of a similar magnitude to those linked to the main aurora (Kotsiaros et al. 2019).

Furthermore, we note an enhancement of B_y around 02:09 UT. Such a bend-forward magnetic field configuration implies a disturbance of the original current system, which may be due to the field-aligned current intensification or plasma ejection (Bunce et al. 2008; Liu et al. 2013).

At Earth, cross-field current disruption also occurs with current sheet expansion (e.g., McPherron et al. 1973; Lui et al. 1988; Angelopoulos et al. 2008; Lui 2011b). Sometimes these two phenomena are not simultaneously observed, i.e., current reduction occurring after current sheet expansion (Yao et al. 2017). However, in this study, we could not determine the sequence of current sheet expansion and total cross-tail current reduction because we were using single-spacecraft measurements.

In summary, we present a middle magnetosphere reconnection event on 2017 May 16 at $\sim 43\,R_J$ by analyzing Juno measurements. We find that this magnetic reconnection event is colocated with a current disruption. Such complex processes could drive intense dynamical electric currents, which may even be of a similar magnitude to currents associated with the main auroral. A statistical study and global magnetospheric simulations would be invaluable for a more comprehensive understanding of whether such a phenomenon in the Jovian magnetosphere is usual or not. Further studies are also needed to understand the difference in magnetospheric dynamics between terrestrial planets (mainly driven by the solar wind) and giant planets (mainly influenced by internal processes).

Acknowledgments

This work was supported by the Fundamental Research Funds for the Central Universities, the National Natural Science Foundation of China (42004149, 42074211). C.S. Arridge and L.C. Ray are supported by an STFC Consolidated Grant to Lancaster University (ST/R000816/1). We are grateful to Frederic Allegrini and Barry H. Mauk for their helpful suggestions. We thank the entire Juno team for the support in using high-quality data. All Juno data presented here are publicly available from NASA's Planetary Data System (https://pds-ppi.igpp.ucla.edu/) as part of the JNO-J-3-FGM-CAL-V1.0 (Connerney 2022), JNO-J/SW-JAD-3-CALIBRATED-V1.0 (Allegrini et al. 2022), and JNO-J-JED-3-CDR-V1.0 (Mauk 2022) data sets for the MAG, JADE, and JEDI instruments. We acknowledge NASA contract NAS5-02099 and V. Angelopoulos for the use of data from the THEMIS Mission. Specifically, we thank K. H. Glassmeier, U. Auster, and W. Baumjohann for the use of FGM data provided under the lead of the Technical University of Braunschweig and with financial support through the German Ministry for Economy and Technology and the German Center for Aviation and Space (DLR) under contract 50 OC 0302. The THEMIS data are available online at http://themis.ssl.berkeley.edu/index.shtml.

ORCID iDs

Dong-Xiao Pan https://orcid.org/0000-0002-0025-3118
Zhong-Hua Yao https://orcid.org/0000-0001-6826-2486
Rui-Long Guo https://orcid.org/0000-0002-7125-0942
Christopher S. Arridge https://orcid.org/0000-0002-0431-6526
Licia C. Ray https://orcid.org/0000-0003-3727-602X
Yong Zhao https://orcid.org/0000-0002-1843-8946
George Clark https://orcid.org/0000-0002-5264-7194
I. Jonathan Rae https://orcid.org/0000-0002-2637-4786
Anthony T. Y. Lui https://orcid.org/0000-0002-6620-2647
Bin-Zheng Zhang https://orcid.org/0000-0002-1555-6023
Yong Wei https://orcid.org/0000-0001-7183-0229
Xu-Zhi Zhou https://orcid.org/0000-0003-4953-1761
Hui-Shan Fu https://orcid.org/0000-0002-4701-7219
John E. P. Connerney https://orcid.org/0000-0001-7478-6462
Scott J. Bolton https://orcid.org/0000-0002-9115-0789

References

Allegrini, F., Wilson, R., Ebert, R., & Loeffler, C. 2022, JUNO J/SW JOVIAN AURORAL DISTRIBUTION CALIBRATED V1.0, JNO-J/SW-JAD-3-CALIBRATED-V1.0, NASA Planetary Data System, doi:10.17189/1519715
Angelopoulos, V., Artemyev, A., Phan, T. D., & Miyashita, Y. 2020, NatPh, 16, 317
Angelopoulos, V., McFadden, J. P., Larson, D., et al. 2008, Sci, 321, 931
Arridge, C. S., Eastwood, J. P., Jackman, C. M., et al. 2016, NatPh, 12, 268
Bunce, E. J., Arridge, C. S., Clarke, J. T., et al. 2008, JGRA, 113, A09209
Connerney, J. 2022, Juno MAG CALIBRATED DATA J V1.0, JNO-J-3-FGM-CAL-V1.0, NASA Planetary Data System, doi:10.17189/1519711
Connerney, J. E. P., Benn, M., Bjarno, J. B., et al. 2017, SSRv, 213, 39
Cowley, S., & Bunce, E. 2001, P&SS, 49, 1067
Delamere, P. A., Otto, A., Ma, X., Bagenal, F., & Wilson, R. J. 2015, JGRA, 120, 4229
Dungey, J. W. 1961, PhRvL, 6, 47
Guo, R. L., Yao, Z. H., Wei, Y., et al. 2018, NatAs, 2, 640
Hill, T. W. 2001, JGR, 106, 8101
Huddleston, D. E., Russell, C. T., Le, G., & Szabo, A. 1997, JGR, 102, 24289
Kivelson, M. G., & Southwood, D. J. 2005, JGRA, 110, A12209
Kotsiaros, S., Connerney, J. E. P., Clark, G., et al. 2019, NatAs, 3, 904
Krupp, N., Vasyliunas, V. M., Woch, J., et al. 2004, in Jupiter: The Planet, Satellites and Magnetosphere, ed. F. Bagenal, T. E. Dowling, & W. B. McKinnon (Cambridge: Cambridge Univ. Press), 617
Liu, J., Angelopoulos, V., Runov, A., & Zhou, X. Z. 2013, JGRA, 118, 2000
Lorch, C. T. S., Ray, L. C., Arridge, C. S., et al. 2020, JGRA, 125, e2019JA027455
Lui, A. T. 2011a, in The Dynamic Magnetosphere, ed. W. Liu & M. Fujimoto (Dordrecht: Springer), 65
Lui, A. T.-Y. 1996, EOSTr, 77, 87
Lui, A. T. Y. 2002, JASTP, 64, 125
Lui, A. T.-Y. 2009, Sci, 324, 1391
Lui, A. T. Y. 2011b, JGRA, 116, A12239
Lui, A. T. Y., Lopez, R. E., Krimigis, S. M., et al. 1988, GeoRL, 15, 721
Makishima, K. 2001, EP&S, 53, 677
Martin, C. J., & Arridge, C. S. 2017, JGRA, 122, 8063
Mauk, B. 2022, JEDI CALIBRATED (CDR) DATA JNO J JED 3 CDR V1.0, NASA Planetary Data System, doi:10.17189/1519713
Mauk, B. H., Haggerty, D. K., Jaskulek, S. E., et al. 2017, SSRv, 213, 289
McComas, D. J., Alexander, N., Allegrini, F., et al. 2017, SSRv, 213, 547
McPherron, R. L., Russell, C. T., Kivelson, M. G., & Coleman, P. J. J. 1973, RaSc, 8, 1059
Miyashita, Y., Miyoshi, Y., Matsumoto, Y., et al. 2005, JGRA, 110, A09S25
Ohtani, S.-i. 2001, SSRv, 95, 347
Paschmann, G., Papamastorakis, I., Sckopke, N., et al. 1979, Natur, 282, 243
Pu, Z. Y., Chu, X. N., Cao, X., et al. 2010, JGRA, 115, A02212
Russell, C., Huddleston, D., Khurana, K., & Kivelson, M. 1999, P&SS, 47, 1101
Russell, C. T., Khurana, K. K., Huddleston, D. E., & Kivelson, M. G. 1998, Sci, 280, 1061
Sarkango, Y., Slavin, J. A., Jia, X., et al. 2021, GeoRL, 48, e2020GL089721
Sarkango, Y., Slavin, J. A., Jia, X., et al. 2022, JGRA, 127, e2021JA030181
Sonnerup, B. U. Ö 1974, JGRA, 79, 1546
Southwood, D. J., & Kivelson, M. G. 2001, JGR, 106, 6123
Vasyliunas, V. M. 1983, in Physics of the Jovian Magnetosphere, ed. A. J. Dessler (Cambridge: Cambridge Univ. Press), 395
Vogt, M. F., Connerney, J. E. P., DiBraccio, G. A., et al. 2020, JGRA, 125, e2019JA027486
Vogt, M. F., Jackman, C. M., Slavin, J. A., et al. 2014, JGRA, 119, 821
Vogt, M. F., Kivelson, M. G., Khurana, K. K., Joy, S. P., & Walker, R. J. 2010, JGRA, 115, A06219
Volwerk, M., André, N., Arridge, C. S., et al. 2013, AnGeo, 31, 817
Yao, Z., Rae, I. J., Lui, A. T. Y., et al. 2017, JGRA, 122, 8560
Yao, Z. H., Bonfond, B., Clark, G., et al. 2020, JGRA, 125, e2019JA027663
Yao, Z. H., Grodent, D., Kurth, W. S., et al. 2019, GeoRL, 46, 11632
Zarka, P. 2007, P&SS, 55, 598
Zweibel, E. G., & Yamada, M. 2009, Annual Reviews, 47, 291